Clays and Clay Minerals, Vol. 42, No. 5, 582–592, 1994.

PALAGONITE RECONSIDERED: PARACRYSTALLINE ILLITE-SMECTITES FROM REGOLITHS ON BASIC PYROCLASTICS

VADIM BERKGAUT,[1] ARIEH SINGER,[1] AND KARL STAHR[2]

[1] The Seagram Centre for Soil and Water Sciences, Faculty of Agriculture
Rehovot 76 100, Israel

[2] Institut für Bodenkunde, Universität Hohenheim
70593 Stuttgart, Germany

Abstract—Poorly crystalline authigenic alteration products of basic pyroclastics from the Golan Heights, Israel, were investigated by XRD, DTA, TGA, FTIR and chemical analysis. Modeling XRD patterns with the use of NEWMOD code provided a way to identify these clays as random interstratified illite/smectites (I/S) with ~70% of illitic interlayers. Their characteristic features were very poor basal reflections, distinct hk bands, high CEC and low (~2%) K_2O content. Crystallite thickness distribution was found to follow Ergun's model with a weight-average thickness of 2.7–2.8 layers. A new method was proposed to calculate the proportion of kaolinite and 2:1 minerals in their mixtures and the average crystallochemical formula of 2:1 minerals in the presence of kaolinite. The method starts from data of chemical analysis and TGA and assumes that the anionic frameworks of kaolinite and 2:1 minerals are exactly $O_{10}(OH)_8$ and $O_{10}(OH)_2$ respectively. The number of OH-groups per ten oxygens not bonded to H in the empirical formula of the mixture is used to evaluate the proportion of kaolinite. Formation of I/S in well-drained environments under humid mediterranean climatic conditions was attributed to long dry seasons. Interstitial water composition was shown to be consistent with authigenic formation of I/S.

Key Words—Basic pyroclastics, Humid mediterranean weathering, Illite/smectite, Poorly-ordered layer silicates.

INTRODUCTION

In a paper entitled; "Mineralogy of palagonitic material from the Golan Heights," Singer (1974) examined the mineralogy of the clay fraction from regoliths derived from basic pyroclastic layers. Among other components such as halloysite, he described a dioctahedral micaceous mineral with well organized crystals along the a and b axes, but with very poor basal reflections, as well as incomplete expansion upon glycolation. This mineral appeared to have formed authigenically from the sideromelanic part of the pyroclastics. In the absence of a better definition, the mineral was termed "palagonite." This term, though not approved by AIPEA Nomenclature Committee, has long been used to denote brown and yellow alteration products of basaltic glass. In a recent review, Singer and Banin (1990) concluded that the mineral most commonly associated with palagonite was smectite, followed by zeolites. Moreover, recent examination showed that the "palagonitic" clay in the Golan Heights occurred not only in water-saturated environments (that are customary for palagonite formation) but also in well drained regoliths that serve as C horizon for soils. The objective of this study was to reexamine the material formerly defined as palagonite and suggest a more appropriate identification.

Intense volcanic activity during the Quaternary in the Golan Heights has given rise in that region to extensive basalt flows, as well as to a series of volcanic cones arranged along two major lines of weakness. The ejected material forming the cones consists of a variety of pyroclastics, including scorias, tuff-lapilli and ash, all of an olivine-basalt composition.

In the northern part of the Golan Heights, the climate is typically humid mediterranean. Rainfall is in the range of 850–950 mm/year, falling in about five winter months, 15% in the form of snow. Summers are long, dry and hot, the average temperature in August reaching 23.4°C and in January, 6.4°C.

MATERIALS AND METHODS

Selected pyroclastic materials (regoliths) were sampled from three volcanic cones (sample B2 from Tel Baron, B3 from Tel Peres and B5 from Tel Shipon) at depths varying between 100–150 cm below surface, from zones that could be regarded as the C horizon of the overlying soils. Soil material (sample B26 from Tel Bental) from the upper horizon of a shallow profile developed on pyroclastics was sampled too. All regolith samples consisted of well-moderately sorted, loosely packed tuff-lapilli particles with diameters ranging between 1–7 mm, cemented by clay and iron oxides. The inner portions of the least weathered larger particles were gray to yellowish, the outer portions, which seemed to consist of clay skins, were dark brown to purple red. The clay content of the regoliths as well as that of the soil ranged between 50–70 wt. %. Water extract pH was neutral to mildly alkaline (7.0–7.6). The fresh rock

Copyright © 1994, The Clay Minerals Society

https://doi.org/10.1346/CCMN.1994.0420511 Published online by Cambridge University Press

Table 1. Extractable Si, Al and Fe and yield of purified clay fractions (wt. % of air-dried <2 μm clay).

Sample	DCB-extractable			NaOH-extractable			Clay fractions, μm		Total recovery %
	SiO_2	Al_2O_3	Fe_2O_3	SiO_2	Al_2O_3	Si/Al	0.1–2	<0.1	
B2	1.28	1.22	4.23	11.86	11.59	0.9	25.7	41.0	97
B3	1.02	0.93	3.73	10.01	8.34	1.0	35.0	34.9	94
B26	0.77	1.20	8.09	10.46	10.01	0.9	30.4	28.7	90
B5	2.29	1.61	4.05	12.38	12.38	0.9	24.4	30.1	87

consisted of forsterite, pyroxenes of the diopside-hedenbergite series, plagioclases and basic volcanic glass (sideromelane) in varying proportions.

The clay mineralogy of the regoliths as well as that of the soils developed on the pyroclastics included kaolinite, halloysite (both 7 and 10 Å forms) and iron oxides, including X-ray crystalline hematite, in addition to the "palagonite" material. Neither allophane nor imogolite were detected by TEM, in accordance with a low content of oxalate-soluble substances (Dan and Singer 1973; Singer 1974; Singer and Navrot 1977; Weller 1992). For the unambiguous identification of the "palagonitic" phase every attempt was made to prepare highly oriented specimens in order to improve its extremely diffuse basal reflections. Consequently, clay fractions were subjected to a series of pretreatments aimed at removing aggregating substances and concentrating the "palagonitic" phase. The following procedure was adopted.

The regolith and soil samples were moistened and gently crushed in the paste state, then the <2 μm fractions were separated by sedimentation in water. The separated clays were treated with 10% H_2O_2 overnight at 60°C, then boiled for ½ hour. Free iron oxides were removed following the procedure of Mehra and Jackson (1960). Suspensions were transferred to centrifuge tubes and washed three times with 0.05 M Na citrate solution, then the clays were treated without drying with 0.5 N NaOH after Hashimoto and Jackson (1960), and the fractions <0.1 μm were separated by centrifugation. Colloidal suspensions of these fractions were yellowish-gold and very transparent. The fine clay fractions were precipitated with Na acetate, centrifuged, and washed once with water and three times with ethanol, each time stirring the sample well with a vortex mixer and shaking for two hours on a reciprocal shaker. Fine and coarse clays were freeze-dried. Major elements extracted by these pretreatments and yields of clay fractions are given in Table 1. According to the Si/Al ratios in the NaOH extracts one can assume that mostly halloysite was dissolved. The separated fine Na-clays produced on glass slides perfect yellowish transparent films with 4–5 mg/cm² thickness and with a high degree of orientation.

In Figure 1, XRD patterns are given for one sample of the untreated bulk clay and of the course and the fine clay subfractions after all pretreatments. It can be observed that hematite was effectively removed by pretreatments and that the coarse clay was enriched in kaolinite. The pattern of the fine clay closely resembled that of the material previously described as "palagonite" (Singer 1974). Therefore <0.1 μm fractions were selected for further detailed examination.

XRD data were obtained using a Philips model 1010 diffractometer with Fe-filtered Co K_α radiation generated at 40 kV and 22 mA, 1° divergence slit, 2 sets of Soller slits and 1 deg/min (2θ) scanning speed. DTA curves were recorded on a Perkin-Elmer DTA 1700 differential thermal analyzer and TGA was carried out on Stanton Redcroft thermal analyzer at a heating rate of 10 deg/min for samples equilibrated at 59% relative humidity. From hygroscopic moisture as determined

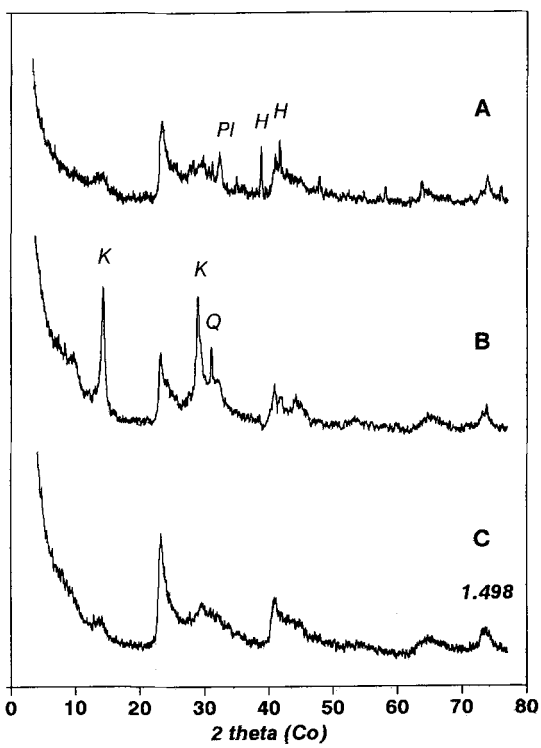


Figure 1. XRD patterns of the untreated <2 μm clay (A) and of the 0.1–2 μm (B) and <0.1 μm (C) clay fractions, separated after H_2O_2, DBC and NaOH pretreatments. Sample B5, unoriented specimens. Pl—plagioclases, H—hematite, K—kaolinite, Q—quartz.

https://doi.org/10.1346/CCMN.1994.0420511 Published online by Cambridge University Press

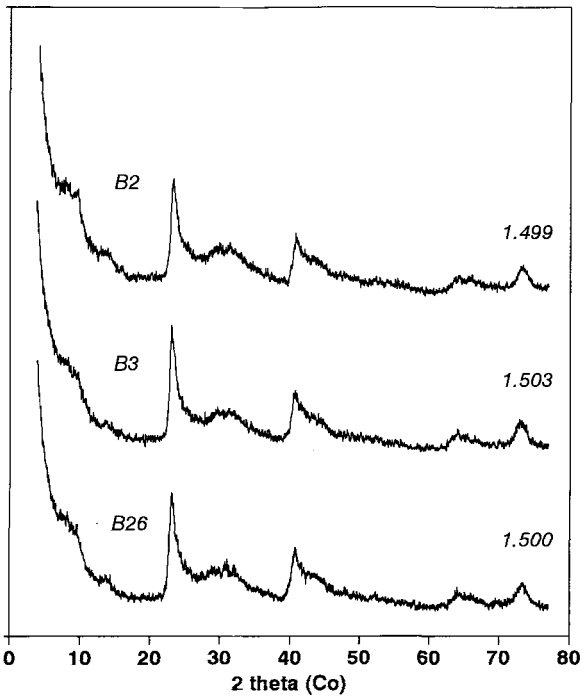


Figure 2. XRD patterns from unoriented specimens of <0.1 μm fractions.

by TGA, rough estimates of specific surface area were calculated, assuming 4.32 molecules of water per a*b area (Reynolds, 1980), or 0.276 mg/m² of water when b = 9 Å. IR spectra were recorded on a Nicolet MX-S FTIR spectrometer using clay/KBr pressed disks heated for 12 h at 150°C. Chemical composition was determined by ICP-AES on a Spectroflame spectrometer produced by Spectro, Germany. Samples were dissolved in HF in tightly capped polyethylene bottles with subsequent addition of H_3BO_3 (Jackson 1974) and standards with the same matrix were used. Cation-exchange capacity of clays was determined by the method of Polemio and Rhoades (1977), except that 0.5 M CH_3COONH_4 solution adjusted to pH 8.2 was used in the replacing step. CEC was also determined using K as saturating cation and drying the samples at 110°C after saturation. Na and K were determined by flame emission spectrometry and Cl on a Jenway model PCLM3 chloridometer.

RESULTS

X-ray diffractometry

The X-ray diffraction patterns of unoriented samples displayed sharp hk bands and broad humps or shoulders instead of sharp 00*l* reflections (Figure 2). In oriented specimens the intensities of the latter strongly increase, while hk bands disappeared (Figure 3). The broad shoulders between 5 and 10° that were present in the patterns of air-dried oriented specimens, disappeared following ethylene glycol solvation, but the strong scattering at low angles persisted. After heating at 350 and 520°C, nearly rational series of broad basal reflections, corresponding to a mica-like structure could be observed. This indicated that the bulk of the samples was composed of extremely thin, platy, easy to orient crystallites of a 2:1 mineral with some expanding interlayers. Two shoulders at 7.3 and 3.57 Å, which disappeared after heating to 520°C, indicated an admixture of kaolinite.

The 06,33 band at 1.499–1.502 Å indicated a dioctahedral structure. The proportion of iron in the octahedral sheet of the 2:1 mineral was deduced from the equation

$$b(\text{Å}) = 8.896 + 0.249\ [(Fe^{+3})/2]$$

(Brigatti 1983),

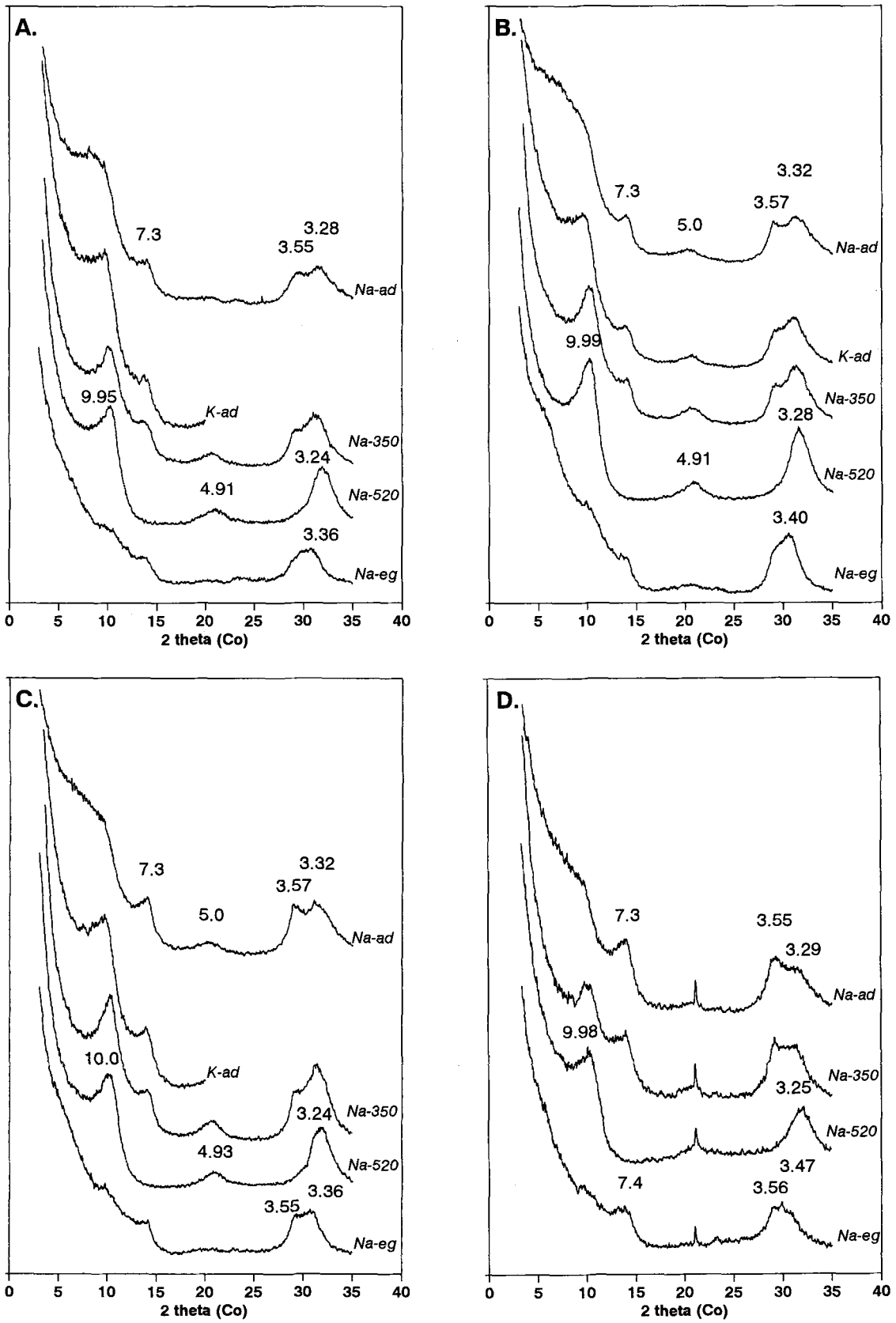
which gave 0.8–0.9 atoms per $O_{10}(OH)_2$. The mean dimension of crystallites along the c-axis was calculated to be ~40 Å after the Scherrer equation ($L = 1/b \cos\theta$) using the half-width of the 003 reflections from the oriented and heated at 520°C specimens. The average crystallite size in the a-b plane was calculated to range between 175–200 Å using the Warren formula ($L = 2l/b \cos\theta$, after Klug and Alexander 1974) from the half-width of the 02,11 bands from random specimens. Corrections for instrumental broadening were made in both cases. An attempt was made to calculate crystallite thickness distribution using an extension of the Warren-Averbach Fourier method developed by Bienenstock, whereby strain broadening is assumed negligibly small (Klug and Alexander 1974). For this purpose the smoothed profile of the 003 reflection of the oriented and 520°C heated specimen of the sample B3 was used. The results after recalculation from number to weight proportions are given in Figure 4. It can be seen that about ⅔ of material is represented by crystallites with only one or two layers, and that thickness distribution fits reasonably well the model of Ergun (1970), according to which the abundances of crystallites diminish exponentially with increasing thickness, shown as a solid line in the figure. The weight-average crystallite thickness from the exponential fit equals 2.8 layers and thus is one layer less than deduced from the Scherrer equation.

To estimate the type of interstratification in the

→

Figure 3. XRD patterns from oriented specimens of <0.1 μm fractions. A—sample B2, B—B3, C—B26, D—B5. Na-ad—air-dried, Na-form; K-ad—air-dried, K-form; Na-350—heated 2 h at 350°C; Na-520—heated 2 h at 520°C; Na-eg—ethylene glycol saturated.

https://doi.org/10.1346/CCMN.1994.0420511 Published online by Cambridge University Press



https://doi.org/10.1346/CCMN.1994.0420511 Published online by Cambridge University Press

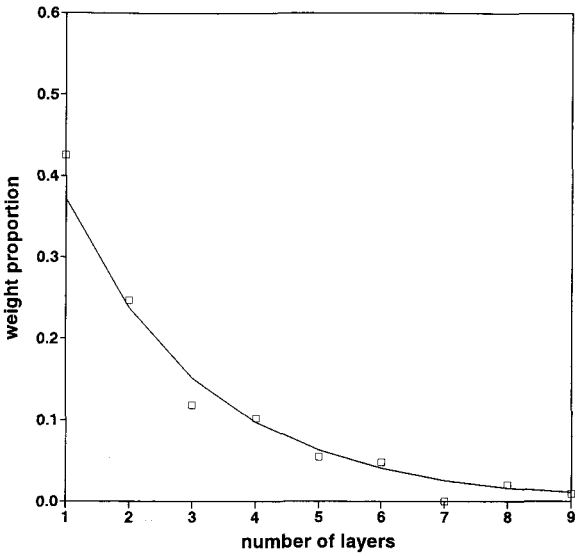


Figure 4. Sample B3, fraction <0.1 μm. Crystalline thickness distribution based on the analysis of the profile of the 003 reflection from the heated at 520°C specimen. Exponential fit according to the Ergun's model is shown by solid line.

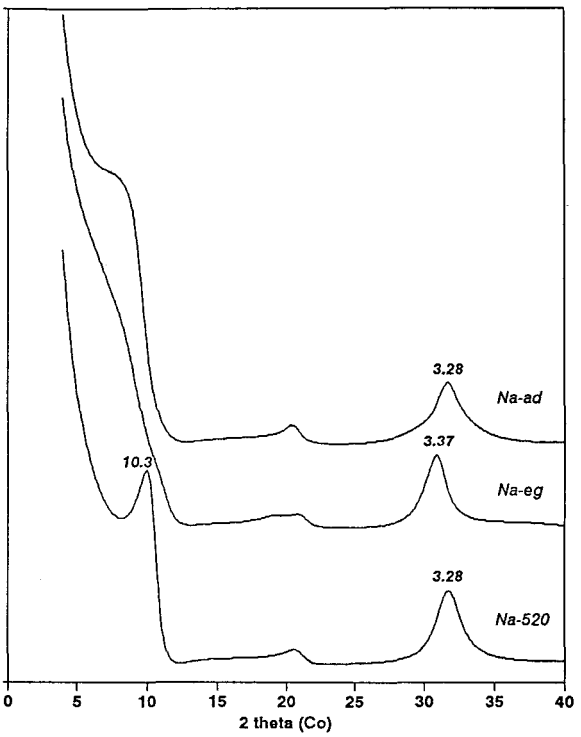


Figure 5. Calculated XRD patterns of the random interstratified illite/smectite with 70% illite interlayers and mean crystallite thickness of 2.8 layers. Crystallite thickness distribution is specified according to Ergun's model. Iron content in octahedral sheet is set to 0.9 atoms per half unit cell. ad—air-dried (50% of illite/smectite—12.5 Å monohydrate and 50% of illite/smectite—15 Å dihydrate), eg—ethylene glycol saturated (50% of expanding interlayers as 14.2 Å single-layer complex and 50% as 16.9 Å two-layer complex), Na-520—heated at 520°C.

structure of the 2:1 mineral the NEWMOD program by Reynolds (1980) was employed. The program was slightly modified to include one layer particles in the distribution of crystallite thicknesses specified by the defect-broadening option and corresponding to Ergun's model. Also modified was the parameter which described this distribution, using the weight-average particle thickness instead of the mean defect-free distance. It was found that a shoulder-shaped 001 reflection was observed only for smectites with a mean crystallite thickness of less than 1.2–1.3 layers, this value corresponding to more than 80% of single layers. In addition, pure smectites did not produce such a noticeable band near 30°. This suggested that the 2:1 mineral under investigation was definitely not a smectite. The observed small departure from the rational series of the d/n values for the specimens heated at 520°C (Figure 3) indicated a mixed layer illite/smectite, and further modeling revealed that XRD patterns from the random interstratified illite/smectite with 60–70% of illite layers (and mean crystallite thickness of 2.7–2.8 layers) had a general shape very similar to the experimental curves, still somewhat differing in peak positions. For the final fit (Figure 5) the probable different states of solvation of the interlayers were taken into consideration: for instance, the band at 3.3 Å from the air-dried specimens was more characteristic for illite/smectite-12.5 Å monohydrate, while the shoulder, instead of the 001 reflection, indicated illite/smectite-15 Å dihydrate. Since NEWMOD did not offer a means of calculating XRD patterns from structures with three different types of layers, calculated curves from illite/smectites with different states of solvation of smectite interlayers were combined. The results were in good agreement with the experiment for 50:50 proportions of mono- and diwater and mono- and di-ethylene glycol expanding interlayers in the air-dried and ethylene glycol solvated state respectively. XRD patterns from air-dried K-saturated specimens (Figure 3) supported the assumption that some vermiculitic interlayers were present.

DTA and FTIR

A strong endothermic peak at 110°C, reflected in a significant weight loss on TGA curves, was due to the removal of hygroscopic water from external surfaces and smectite interlayers of crystallites (Figures 6 and 7). Dehydroxylation occurred at 470–480°C. This temperature is characteristic for both poorly crystalline kaolinite and smectites with the iron content as estimated from XRD data (Brigatti 1983). The weak, diffuse exothermic peak at 870°–880°C corresponds to recrystallization of metakaolinite to mullite.

FTIR spectra were also consistent with XRD data and demonstrated a good short-range order of the in-

https://doi.org/10.1346/CCMN.1994.0420511 Published online by Cambridge University Press

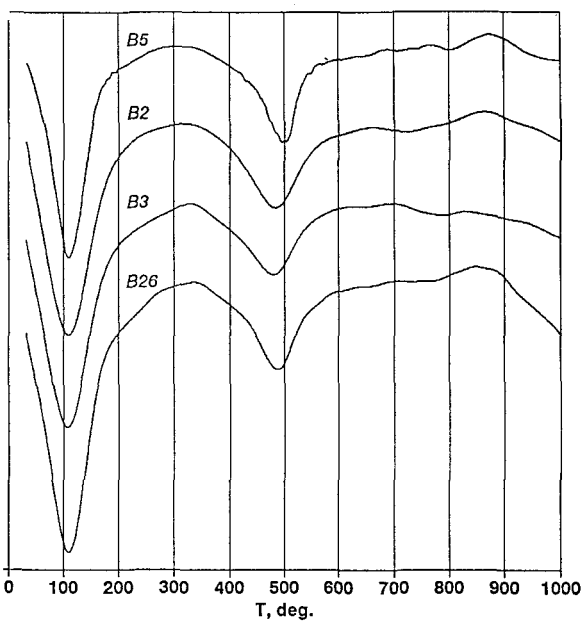


Figure 6. DTA-curves of <0.1 μm fractions.

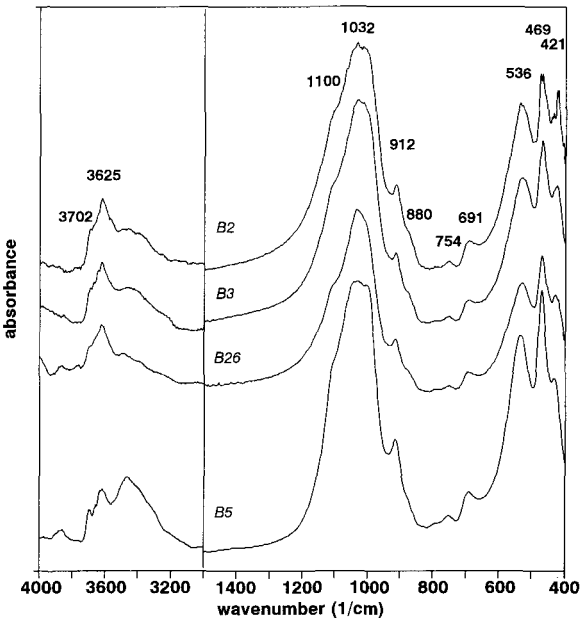


Figure 8. IR spectra of <0.1 μm fractions.

vestigated clays (Figure 8). The shoulder at 3702 cm^{-1} (stretching band of surface internal OH-groups of kaolinite) demonstrated that this mineral is present but not dominant. An AlAlOH deformation band at 912 cm^{-1} is equally characteristic for 1:1 and 2:1 dioctahedral minerals, but again this band would be significantly stronger if 1:1 structures were prevalent. The proportion of iron in octahedral layers of 2:1 minerals is sufficient to give a shoulder at 870 cm^{-1} (deformation of Fe^{+3} AlOH grouping) but not so significant as in nontronites so as to produce the band at 815 cm^{-1}, corresponding to $Fe^{+3}Fe^{+3}OH$. The 400–600 cm^{-1} region is typical for phengite-type illite.

The spectra of the samples heated for two hours at 520°C (not shown) revealed that all hydroxyl groups had been lost during that treatment.

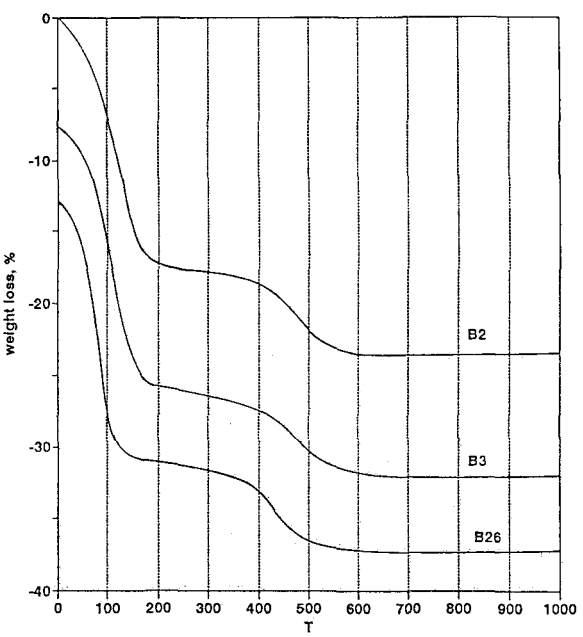


Figure 7. TGA-curves of <0.1 μm fractions.

Chemical composition and quantitative determination of the phases

TGA together with chemical analysis provide a sound basis for the quantitative determination of clay composition, being least subject to the order-disorder in the structures of clay minerals. The method described below assumes only that the stoichiometry of the anionic skeleton is constant and is represented by $O_{10}(OH)_8$ for kaolinite and by $O_{10}(OH)_2$ for 2:1 minerals. Such an assumption seems to be justified by the long-term practice of calculating structural formulas for pure clay minerals. Minerals known to deviate from this stoichiometry are rare, as an example Fe^{+3}-oxisaponite with a significant lack of OH-groups can be mentioned (Drits and Kossovskaya 1990).

The source data for the calculations was chemical composition, including water of OH-groups from TGA determinations, on the hygroscopic moisture free basis (Table 2). All the water removed before the beginning of dehydroxylation endothermic reaction, as estimated from DTA curves, was considered as hygroscopic. TiO_2, P_2O_5 and CaO were supposed to be incorporated in non-clay impurities, such as rutile, anatase, sphene and

https://doi.org/10.1346/CCMN.1994.0420511 Published online by Cambridge University Press

Table 2. Calculation of mineralogical composition of <0.1 μm fraction (sample B2).

	Na_2O	K_2O	SiO_2	Al_2O_3	Fe_2O_3	MgO	MnO_2	H_2O	Σ
Chemical composition, oxides on ignited basis, water of OH-groups by TGA on hygroscopic moisture-free basis, Ca, P, and Ti excluded	2.51	1.78	51.28	27.42	12.38	2.43	0.05	7.57	
Chemical composition, on hygroscopic moisture-free basis	2.32	1.65	47.40	25.34	11.44	2.25	0.05	7.57	98.01
Empirical formula	$Na_{0.075}K_{0.035}Si_{0.789}Al_{0.497}Fe_{0.143}Mg_{0.056}Mn_{0.001}O_{3.070}H_{0.840}$ or $Na_{0.075}K_{0.035}Si_{0.789}Al_{0.497}Fe_{0.143}Mg_{0.056}Mn_{0.001}O_{2.230}(OH)_{0.840}$								
Empirical formula with 10O atoms	$Na_{0.34}K_{0.16}Si_{3.54}Al_{2.23}Fe_{0.64}Mg_{0.25}O_{10}(OH)_{3.77}$								
Resolution into $O_{10}(OH)_8$ and $O_{10}(OH)_2$ minerals (mole proportion of kaolinite on $O_{10}(OH)_8$ basis = (3.77 − 2)/6)	0.30 mole parts of $Al_4Si_4O_{10}(OH)_8$ + 0.70 mole parts of $Na_{0.48}K_{0.22}Si_{3.34}Al_{1.49}Fe_{0.91}Mg_{0.35}O_{10}(OH)_2$								
Crystallochemical formula for 2:1 mineral	$Na_{0.48}K_{0.22}[Si_{3.34}Al_{0.66}][Al_{0.83}Fe_{0.91}Mg_{0.35}]O_{10}(OH)_2$								

Weight proportion of kaolinite = $0.30 \cdot MM(Al_4Si_4O_{10}(OH)_8)/MM(Na_{0.34}K_{0.16}Si_{3.54}Al_{2.23}Fe_{0.64}Mg_{0.25}O_{10}(OH)_{3.77}) \cdot 98.01\%$ = 33.9%, where MM = molecular mass corresponding to a formula in parentheses.

apatite, and therefore excluded (Bain and Smith 1987). The empirical formula of the mixture was calculated and normalized on $O_{10}(OH)_x$ basis. From this x the mole proportion of kaolinite in the mixture can be determined. If m denotes mole proportion of kaolinite (on $O_{10}(OH)_8$ basis) and 1 − m is the mole proportion of 2:1 mineral (on $O_{10}(OH)_2$ basis), then the mixture should have 8m + 2(1 − m) hydroxyl groups per 10 oxygens not bonded to H, whence m = (x − 2)/6. From the mole proportion of kaolinite its weight proportion was calculated. The average crystallochemical formula for 2:1 minerals was obtained as usual, assuming Si only in tetrahedral, Al both in tetra- and octahedral, Fe^{+3} and Mg only in octahedral positions.

The errors in the calculated values can originate from the errors in chemical analysis, in thermogravimetric determination of water of OH-groups, and from unaccounted impurities. The last two sources of errors are probably the most important. The uncertainty in the measurement of the weight loss due to dehydroxylation arise from the uncertainty of the temperature range, in which dehydroxylation occurs, because both before and after the reaction the weight of a sample does not remain exactly constant (Figure 7). In order to check how these factors can influence the final results, the same calculations as shown in Table 2 were performed, allowing 5% variation of the content of dehydroxylation water from the experimentally determined value. In addition, calculations were carried out allowing 5% of quartz, albite or hematite as unaccounted impurities. From the results shown in Table 3, it can be seen that calculated proportion of kaolinite was not very sensitive to such variations in source data and did not change more than 11% relative. It should be remembered that in quantitative mineralogical analysis, especially of clays, results within 10% relative or 3% absolute are considered as "highly accurate" (Pevear 1989). The calculated crystallochemical formulas of 2:1 minerals were generally more sensitive to unaccounted impurities than to errors in TGA, but the calculated sum of octahedral cations remained remarkably uniform.

This method could be directly applied to the present samples since they contained no quartz, and amorphous compounds and free iron oxides were removed by pretreatments. The results of the calculations are shown in Table 4. They confirm that the investigated clays consist mostly of a high-charged, iron-rich dioctahedral 2:1 mineral. The estimates of iron content in octahedral layers are in perfect agreement with the assessments derived from XRD. At first glance it would seem that the K_2O content was too low for an illite/

Table 3. Variability of calculated mineralogical composition in relation to errors in TGA determinations and in the presence of unaccounted impurities (sample B2).

Water of OH-groups, wt. %	Unaccounted impurities, wt. %	Calculated mineralogical composition			
		Kaolinite, wt. %	Formula for 2:1 mineral	$\Sigma_{oct.}$	$\Sigma_{interlayer}$
7.57	—	33.9	$Na_{0.48}K_{0.22}[Si_{3.34}Al_{0.66}][Al_{0.83}Fe_{0.91}Mg_{0.35}]O_{10}(OH)_2$	2.10	0.70
7.95 (+5%)	—	37.7	$Na_{0.51}K_{0.24}[Si_{3.36}Al_{0.64}][Al_{0.74}Fe_{0.97}Mg_{0.38}]O_{10}(OH)_2$	2.09	0.74
7.19 (−5%)	—	30.1	$Na_{0.45}K_{0.21}[Si_{3.33}Al_{0.67}][Al_{0.92}Fe_{0.86}Mg_{0.33}]O_{10}(OH)_2$	2.11	0.66
7.57	5% quartz	36.9	$Na_{0.55}K_{0.26}[Si_{3.11}Al_{0.89}][Al_{0.68}Fe_{1.06}Mg_{0.41}]O_{10}(OH)_2$	2.16	0.81
7.57	5% albite	36.7	$Na_{0.41}K_{0.26}[Si_{3.28}Al_{0.73}][Al_{0.70}Fe_{1.05}Mg_{0.41}]O_{10}(OH)_2$	2.15	0.66
7.57	5% hematite	35.6	$Na_{0.52}K_{0.24}[Si_{3.55}Al_{0.45}][Al_{1.08}Fe_{0.56}Mg_{0.39}]O_{10}(OH)_2$	2.02	0.76

https://doi.org/10.1346/CCMN.1994.0420511 Published online by Cambridge University Press

Table 4. Chemical and mineralogical composition of <0.1 μm fractions.

	B2	B3	B26
Al_2O_3	27.42	24.98	25.71
MnO_2	0.05	0.04	0.06
MgO	2.43	2.63	3.13
K_2O	1.78	1.78	1.77
SiO_2	51.28	51.93	52.14
Fe_2O_3	12.38	13.12	12.34
P_2O_5	0.09	0.10	0.09
CaO	0.20	0.24	0.35
TiO_2	1.85	2.06	1.88
Na_2O	2.51	3.11	2.52
$H_2O(OH)$	7.57	7.90	7.49
l.o.i.	24.75	23.75	24.00
Kaolinite	33.9	38.0	33.0
2:1 mineral	64.3	60.0	65.1
composition of 2:1 mineral			
Si^{IV}	3.34	3.46	3.41
Al^{IV}	0.66	0.54	0.59
Al^{VI}	0.83	0.55	0.73
Fe^{VI}	0.91	1.07	0.91
Mg^{VI}	0.35	0.41	0.45
Σ_{oct}	2.09	2.03	2.09
Na	0.48	0.64	0.47
K	0.22	0.24	0.22
$\Sigma_{interlayer}$	0.70	0.88	0.69

Oxides on ignited basis; water of OH-groups on hygroscopic moisture-free basis, by TGA; loss on ignition on the basis of a sample, equilibrated at 59% relative humidity, by TGA.

smectite with 60–70% of illite layers, but actually it also agrees well with the model based on the XRD data. From this model K_2O content should be approximately equal to $10\% \cdot 0.65 \cdot 0.7 \cdot \Sigma\, p_i(i - 1)/i = 2.0\%$, where 10% is the concentration of K_2O in pure illite, 0.65 is the proportion of the mixed layered 2:1 mineral, 0.7 is the proportion of the illite interlayers in it, p_i is the weight proportion of crystallites with the thickness of i layers, and $(i - 1)/i$ allows for the depletion of K from external surfaces. The calculated average layer charge is also by and large consistent with ~30% of smectite interlayers as estimated from XRD data, from which it comes out to $0.3 \cdot 0.3 + 0.7 \cdot 0.9 = 0.72$, assuming charges of 0.3 and 0.9 per $O_{10}(OH)_2$ for smectite and illite respectively. The high proportion of external surfaces due to the small particle thicknesses also contributes significantly to the high CEC and specific surface area (SSA) of the investigated materials (Table 5). From the model based on XRD data SSA of the mixed-layered 2:1 mineral should be equal to $810 \cdot \Sigma\, p_i[(1/i) + 0.3(1 - 1/i)] = 585$ m²/g, where 810 m²/g is the SSA of pure smectite, 0.3 is the proportion of smectitic interlayers and $1/i + 0.3(1 - 1/i)$ term allows for external surfaces of crystallites. It should be remembered though that the values for SSA in Table 5 are but rough approximates.

Table 5. Cation exchange capacity and specific surface area of <0.1 μm fractions.

Sample	CEC, meq/100 g Na[1]	CEC, meq/100 g K[1]	SSA, m²/g
B2	80	66	636
B3	74	68	665
B26	70	65	656

CEC on the air-dry basis; SSA calculated from hygroscopic moisture at 59% relative humidity.

[1] Saturating cation.

DISCUSSION

In the previous section the 2:1 mineral under investigation was described as interstratified illite/smectite with an unusually low mean particle thickness. But the concept of interstratification applied to such a finely divided material could be rather confusing. Since XRD directly measures interlayer spacings and not layer charges, it cannot distinguish between single-layer illite and smectite. In particles with two 2:1 layers, interlayers can be either illitic or smectitic. This means that the description of a clay mineral as a mixed-layer is directly applicable only to those with sufficiently thick particles. The investigated 2:1 layer silicate can also be characterized according to XRD data as a mixture of a single-layer 2:1 mineral with unknown charge (which produced the diffuse strong scattering at low angles from the oriented specimens), individual double-layer illite, individual double-layer smectite and "true" interstratified illite/smectite, the latter comprising about ⅓ by weight.

One may anticipate that clays with even higher proportion of one-layer thick crystallites could be encountered. For such materials the usual procedure of X-ray identification turns out to be unsuitable, since no basal reflections are observed. Probably if X-ray scattering at low angles strongly enhances upon orientation, it could be a good indication for the presence of single-layer crystallites.

Another problem arising is why there is no interparticle diffraction in case of the investigated illite/smectites, or at least why it is strongly reduced. One possible explanation in the context of fundamental particles theory (Nadeau *et al* 1984) is that two kinds of fundamental particles could exist, behaving differently during the preparation of oriented specimens. The properties of fundamental particles regulating such behavior remain obscure. Another explanation of course is that this theory is wrong and that a smectite interlayer, once broken, does not reestablish to give interparticle diffraction, and that the discrepancy between XRD and TEM data is probably due to the number of smectite interlayers broken during laboratory preparation.

Generally speaking, the poor crystallinity of clays

https://doi.org/10.1346/CCMN.1994.0420511 Published online by Cambridge University Press

Table 6. Interstitial water composition, Tel Avital pyroclastic cone (from Singer *et al* 1991).

Sample	pH	Si	Al	Fe	Ca ppm	Mg	Na	K
Middle black unit	6.85	33.5	0.16	4.35	12.7	2.8	17.7	3.1
Upper mixed unit	6.80	29.1	0.13	2.09	22.6	4.3	22.7	5.7

formed from volcanic ash is probably due to the high rates of weathering of pyroclastic materials. It had been shown in laboratory experiments that volcanic glass dissolved 1.5–2.5 orders of magnitudes faster than calcic plagioclases and olivine, and 1–1.5 orders of magnitude faster than crystalline basalt (Gislason and Eugster 1987). Because of this and because kinetics of precipitation is slow for aluminosilicates, a high degree of supersaturation can develop, leading to precipitates with extremely small and imperfect crystals. According to Ostwald's rule, the least thermodynamically stable phases, namely allophane and imogolite, tend to precipitate first and can persist for several thousand years in soils on recent volcanic deposits (Wada 1987) before being replaced by more stable layer silicates. This crystallization sequence has been reproduced under laboratory conditions (Kawano and Tomito 1992), and it was found that pH above 7 promoted the transformation of allophanes to layer silicates (Farmer *et al* 1991a, 1991b). Therefore in the pyroclastic-derived soils of the Golan Heights, allophanes should have been ephemeral, and they are absent from these soils at present (Singer and Navrot 1977).

Soils on volcanic ashes and pumice have been mostly described in the areas of recent volcanic activity and temperate humid climate and have allophanes and halloysite as predominant secondary minerals (Wada 1987). There is much evidence that under drier conditions smectite can form authigenically in well-drained pumiceous soils. Wada *et al* (1990) identified smectite as one of the major clay minerals derived from basic volcanic ashes on the island of Hawaii. Quantin *et al* (1975) reported the formation of smectite in soils formed under dry conditions in the New Hebrides. Mizota and Chapelle (1988) reported halloysite and "curved smectite" in soils derived from basic volcanic ashes under udic marginal to ustic moisture regimes in Rwanda, Central Africa. At least in some of the profiles, smectite seemed to be a major weathering product (Van der Gaast *et al* 1986; Mizota 1987). A particular type of smectite with a curly morphology was detected, displaying distinct hk bands, but very weak basal reflections, caused, according to the authors, by poor layer stacking. This material thus resembles to some degree the "palagonite" described from the Golan Heights.

Existing views on the possibility of mica formation under soil conditions are somewhat controversial. This process is believed to happen in soils of arid climate, but usually is hard to prove because illite can be inherited from parent materials or introduced from the outside by aeolian processes. Illite occurrences in the pyroclastic derived soils of the Golan Heights has been attributed to inputs from aeolian dust (Singer and Navrot 1977). Mica synthesis was proposed for certain high rainfall soils of Hawaii, but subsequently it was shown to be of aeolian origin (See the review of Fanning *et al* 1989). In Canary Islands soils developed on pyroclastics, illite presence was explained by an illitization of pedogenic smectite, with the K introduced by sea spray (Jahn *et al* 1987). Immature ash soils found in western Sudan by White (1967) contained kaolinite, illite and clay-size quartz. Mica, the major component in the clay fractions in the pyroclastic derived soils with an aridic moisture regime from the Ngoro Ngoro Crater, Tanzania, was first believed to be of aeolian origin (Mizota *et al* 1988). Oxygen isotope analysis, however, suggested its pedogenic formation.

Layer silicates were not detected in unweathered tuff-lapilli of the Golan Heights, and aeolian contamination is unlikely for unexposed weathered regoliths completely preserving the structure of original pyroclastic rock. Quartz, shown to be a good tracer for aeolian inputs (Singer and Navrot 1977), is nearly absent from the regoliths, adding support that they were never affected by aeolian conditions. Therefore the illite/smectites under investigation should have been formed *in situ*.

Probably the most important factor favoring illite/smectite formation in the pyroclastic-derived regoliths of the Golan Heights is the prolonged dry summer. Halloysite and kaolinite may form during wet season, while illite-smectite may precipitate during desiccation of soils and regoliths from waters entrapped in pumice pores. In such microenvironments concentrations of Si and bases should increase significantly as a result of a longer rock-water interaction and evaporatory concentration. The same factor is favorable for the crystallization of hematite, which was detected in DCB-untreated clays (Figure 1). Another process possibly involved is an irreversible smectite-to-illite transformation of K-smectite, or smectite in presence of K-bearing minerals, in wetting and drying cycles. This process was investigated in detail under laboratory conditions and is considered to be of a great geological importance (Srodon and Eberl 1984).

The composition of interstitial waters sampled at the end of dry season from one of the volcanic cones sup-

https://doi.org/10.1346/CCMN.1994.0420511 Published online by Cambridge University Press

ports the suggestion that present-day illite/smectite formation is possible in pyroclastic-derived regoliths. Waters contained about 70 ppm SiO_2 and 3–6 ppm K (Table 6), these values placing the composition near the triple kaolinite-smectite-illite phase joint (Garrels 1984). However, this result should be treated with caution, since the referred stability diagram deals with SiO_2-Al_2O_3-K_2O-H_2O system. Regrettably, thermodynamic data for iron-bearing illites and smectites are not available at present. Still the concentrations of K are in the range where dioctahedral micas rather take than release K into solution (Fanning *et al* 1989).

CONCLUSIONS

A combination of analytical methods was used to characterize dioctahedral 2:1 mineral formed authigenically from basic pyroclastic deposits of the Golan Heights in association with halloysite and hematite. This mineral produced very poor basal X-ray diffraction reflections, but strong sharp hk bands in specimens with random orientation. From oriented 520°C heated specimens nearly rational series of broad basal reflections, corresponding to a mica-like structure was observed. Diffracted intensity from air-dried and ethylene glycol saturated specimens strongly increased below 10° upon orientation, but no distinct 001 reflections appeared. These unusual properties were attributed to the low mean crystallite thickness of the 2:1 mineral. Calculated crystallite thickness distribution followed Ergun's model with 2.7–2.8 layers weight average thickness. This corresponded to ⅔ by weight of crystallites having only one or two layers. Using NEWMOD code, this mineral was identified as random interstratified illite/smectite with ~70% of illitic interlayers. In spite of the high proportion of illitic interlayers, CEC, specific surface and K_2O content were closer to those of smectite, due to the contribution of external surfaces of crystallites. A new method was used to calculate crystallochemical formulas of 2:1 minerals in the presence of kaolinite from the data of chemical analysis and TGA, based on the resolution of the empirical formula of the mixture into minerals with $O_{10}(OH)_8$ and $O_{10}(OH)_2$ anionic frameworks. The results were shown to be not very sensitive to errors in source data and to unaccounted impurities. A typical formula thus obtained was $Na_{0.48}K_{0.22}$ $[Si_{3.34}Al_{0.66}]$ $[Al_{0.83}Fe^{3+}_{0.91}Mg_{0.35}]$ $O_{10}(OH)_2$. The formation of illite/smectite under humid mediterranean climatic conditions was attributed to long dry seasons, and its poor crystallinity to high rates of weathering of volcanic glass. The composition of water sampled at the end of dry season conformed with the present-day formation of illite/smectite.

ACKNOWLEDGMENT

The authors gratefully acknowledge the financial assistance extended to them within the framework of the University of Hohenheim, Germany, and Faculty of Agriculture, Hebrew University, Israel, Agreement of Cooperation.

REFERENCES

Bain, D. C., and B. F. L. Smith. 1987. Chemical analysis. In *A Handbook of Determinative Methods in Clay Mineralogy.* M. J. Wilson, ed. Glasgow and London: Blackie, New York: Chapman and Hall, 248–274.

Brigatti, M. F. 1983. Relationships between composition and structure in Fe-rich smectites. *Clay Miner.* **18**: 177–186.

Dan, J., and A. Singer. 1973. Soil evolution on basalt and basic pyroclastic materials in the Golan Heights. *Geoderma* **9**: 165–192.

Drits, V. A., and A. G. Kossovskaya. 1990. *Clay Minerals: Smectites and Interstratified Mica-Smectites and Chlorite-Smectites.* Moscow: "Nauka," 245 pp. [in Russian].

Ergun, S. 1970. X-ray scattering by very defective lattices. *Phys. Rev.* **B1**: 3371.

Fanning, D. S., V. Z. Keramidas, and M. A. El-Desoky. 1989. Micas. In *Minerals in Soil Environments,* 2nd ed. J. B. Dixon and S. B. Weed, eds. Madison: SSSA, 551–634.

Farmer, V. C., W. J. McHardy, F. Palmieri, A. Violante, and P. Violante. 1991a. Synthetic allophanes formed in calcareous environments. Nature, conditions of formation and transformations. *Soil Sci. Soc. Amer. J.* **55**: 1162–1166.

Farmer, V. C., G. S. R. Krishnamurti, and P. M. Huang. 1991b. Synthetic allophane and layer-silicate formation in SiO_2-Al_2O_3-FeO-Fe_2O_3-MgO-H_2O systems at 23°C and 89°C in a calcareous environment. *Clays & Clay Miner.* **39**: 561–570.

Garrels, R. M. 1984. Montmorillonite/illite stability diagrams. *Clays & Clay Miner.* **32**: 161–166.

Gislason, S. R., and H. P. Eugster. 1987. Meteoric water-basalt interaction. I: A laboratory study. *Geochim. Cosmochim. Acta* **51**: No. 10, 2827–2840.

Hashimoto, I., and M. L. Jackson. 1960. Rapid dissolution of allophane and kaolinite-halloysite after dehydration. *Clays & Clay Miner.* **7**: 102–113.

Jahn, R., M. Zasei, and K. Stahr. 1987. Formation of clay minerals in soils developed from basic volcanic rocks under semi-arid climatic conditions in Lanzarote, Spain. *Catena* **14**: 359–368.

Jackson, M. L. 1974. *Soil Chemical Analysis—Advanced Course,* 2nd ed. Madison: Published by the author, 895 pp.

Kawano, M., and K. Tomita. 1992. Formation of allophane and beidellite during hydrothermal alteration of volcanic glass below 200°C. *Clays & Clay Miner.* **40**: 666–674.

Klug, H. P., and L. E. Alexander. 1974. *X-ray Diffraction Procedures for Polycrystalline and Amorphous Materials.* Wiley, New York, 664 pp.

Mehra, O. P., and M. L. Jackson. 1960. Iron oxide removal from soils and clays by a dithionite-citrate system buffered with sodium bicarbonate. *Clays & Clay Miner.* **7**: 317–327.

Mizota, C. 1987. Chemical and mineralogical characterization of soils derived from volcanic ashes. In *Agriculture and Soils in Kenya. A Case Study of Farming Systems in the Embu District and Characterization of Volcanogenous Soils.* S. Hirose, ed. Tokyo: College of Agric. and Veter. Medicine, Nihon Univ., 110–123 [in Japanese].

Mizota, C., and J. Chapelle. 1988. Characterization of some Andepts and Andic soils in Rwanda, Central Africa. *Geoderma* **43**: 131–141.

Mizota, C., I. Kawasaki, and T. Wakatsuki. 1988. Clay mineralogy and chemistry of seven pedons formed on volcanic ash, Tanzania. *Geoderma* **43**: 131–141.

Mizota, C., and L. P. Reeuwijk. 1989. *Clay Mineralogy and*

https://doi.org/10.1346/CCMN.1994.0420511 Published online by Cambridge University Press

Chemistry of Soils Formed in Volcanic Material in Diverse Climate Regions. Soil Monograph 2, ISRIC, Wageningen, Holland.

Moore, D. M., and R. C. Reynolds Jr. 1989. *X-Ray Diffraction and Identification and Analysis of Clay Minerals.* Oxford, New York: Oxford Univ. Press, 332 pp.

Nadeau, P. H., J. M. Tait, W. J. McHardy, and M. J. Wilson. 1984. Interstratified XRD characteristics of physical mixtures of elementary clay particles. *Clay Miner.* **19**: 67–76.

Pevear, D. R. 1989. Introduction. In *CMS Workshop Lectures, Vol. 1, Quantitative Mineral Analysis of Clays.* D. R. Pevear and F. A. Mumpton, eds. Evergreen, Colorado: The Clay Minerals Society, 1–2.

Polemio, M., and J. D. Rhoades. 1977. Determining cation exchange capacity. A new procedure for calcareous and gypsiferous soils. *Soil Sci. Soc. Amer. J.* **41**: 524–528.

Quantin, P., D. Badaut-Trauth, and F. Weber. 1975. Mise en evidence de mineraux secondaires, argiles et hydroxides, dans les andosols des Nouvelles-Hebrides, apres la deferrification par la methode de Endredy. *Bull. Groupe franc. Argiles* **27**: 51–67.

Reynolds, R. C. 1980. Interstratified clay minerals. In *Crystal Structures of Clay Minerals and Their X-ray Identification.* G. W. Brindley and G. Brown, eds. London: Mineralogical Society, 249–304.

Singer, A. 1974. Mineralogy of palagonitic material from the Golan Heights, Israel. *Clays & Clay Miner.* **22**: 231–240.

Singer, A., and J. Navrot. 1977. Clay formation from basic volcanic rocks in a humid Mediterranean climate. *Soil Sci. Soc. Amer. J.* **41**: No. 3, 645–650.

Singer, A., A. Silber, and D. Szafranek. 1991. Nodular silica-phosphate minerals of the Har Peres pyroclastics, Golan Heights. *N. Jb. Miner. Mh. Jg.* **H.8**: 337–354.

Singer, A., and A. Banin. 1990. Characteristics and mode of formation of palagonite—A review. In *Proc. 9th Int. Clay Conf., Strasbourg, 1989.* V. C. Farmer and Y. Tardy, eds. *Sci. Gwol., Mwm.* **88**: 173–181.

Srodon, J., and D. D. Eberl. 1984. Illites. In *Micas.* S. W. Bailey, ed. Chelsea, Michigan: Mineralogical Soc. of America, 495–544.

Van der Gaast, S. J., C. Mizota, and J. H. F. Jansen. 1986. Curved smectite in soils from volcanic ash in Kenya and Tanzania. A low angle X-ray powder diffraction study. *Clays & Clay Miner.* **34**: 665–671.

Wada, K. 1987. Minerals formed and mineral formation from volcanic ash by weathering. *Chem. Geol.* **60**: 17–28.

Wada, K., Y. Kakuto, and H. Ikawa. 1990. Clay minerals of two Eutrandepts of Hawaii, having isohyperthermic temperature and ustic moisture regimes. *Soil Sci. Soc. Amer. J.* **54**: 1173–1178.

Wada, K. 1980. Mineralogical characteristics of Andisols. In *Soils and Variable Charge.* B. K. G. Theng, ed. Lower Hutt, New Zealand: Soil Bureau, 87–109.

Weller, U. 1992. *Bodenentwicklung und Tonmineralbildung aus vulkanischem Tuff auf den Golanhöhen.* Israel: Diplomarbeit, Universität Hohenheim, 60 pp.

White, L. P. 1967. Ash soils in Western Sudan. *J. Soil Sci.* **18**: No. 2, 309–317.

(Received 22 November 1993; accepted 28 April 1994; Ms. 2440)

https://doi.org/10.1346/CCMN.1994.0420511 Published online by Cambridge University Press